Decoupled Design of Controllers for Aerial Manipulation with Quadrotors

Pedro O. Pereira, Riccardo Zanella and Dimos V. Dimarogonas

***Abstract*— In this paper, we model an aerial vehicle, specifically a quadrotor, and a load attached to each other by a rigid link. We assume a torque input at the joint between the aerial vehicle and the rigid link is available. After modeling, we decouple the system dynamics in two separate subsystems, one concerning the position of the center of mass, which we control independently from the chosen torque input; and a second subsystem, concerning the attitude of the rigid link, which we control by appropriately designing a torque control law. Differential flatness is used to show that controlling these two separate systems is equivalent to controlling the complete system. We design control laws for the quadrotor thrust, the quadrotor angular velocity and the torque input, and provide convergence proofs that guarantee that the quadrotor follows asymptotically a desired position trajectory while the manipulator follows a desired orientation. Simulation and experimental works are presented which validate the proposed algorithms.**

I. Introduction

Aerial transportation, concerning the execution of complex manipulation tasks in unstructured and dynamic environments, is an active topic of research in robotics. Compared to ground robots, aerial robots allow for manipulation tasks to be executed in difficult to access spaces, opening the doors to new applications, such as the inspection and maintenance of aging infrastructures [1]. Multi-rotor helicopters, and in particular quadrotors, are preferred to others types of UAVs owing to their capability to hover, to take off and land vertically, to their high manoeuvrability, and to the availability of inexpensive components. Also, several position trajectory tracking controllers for quadrotors are found in the literature [2].

Different forms of manipulation with aerial vehicles are found in the literature, and most take advantage of trajectory tracking controllers for quadrotors such as those found in [2]. One approach to aerial manipulation is to suspend an object by a cable, in which case controlling the sway between the object and the UAV is necessary. In [3], the problem of lifting a cable-suspended load with unknown mass from the ground proceeded by transporting such load is studied. In [4], the sway of the suspended load is minimized by means of a trajectory optimization, while in [5] an adaptive controller is presented that avoids swing excitation. In [6], the problem of controlling multiple robots manipulating and transporting a common load via cables is addressed. Manipulation by means of cable suspension is limited, in the sense that the load's position relative to the transporting UAV depends on the trajectory the load is required to track.

An alternative manipulation task is by means of a gripper. In [7], [8], a gripper is installed under a UAV that grasps, holds and transports an object . Carrying an external load rigidly attached to the UAV body through a gripper changes the flight characteristics of the aerial vehicle, such as the inertia of the system, and [8] provides bounds on the controller gains that guarantee that stability is preserved when a load is gripped. In [9], the problem of high-speed grasping and transportation of loads is studied, and it draws inspiration from aerial hunting by birds of prey. In [10], a team of quadrotors are employed to collaboratively pick up an object using a similar gripper.

An alternative to a gripper is a robotic manipulator with actuated joints, which provide additional degrees of freedom [11]. Control strategies for UAVs with robotic manipulators are found that consider the UAV and manipulator as two independent subsystems, and their coupling is seen as an external disturbance to each other. In [12], [13], the controller considers the variation of the center of mass position and of the inertia matrix caused by the manipulator motion. A task-based control strategy is proposed in [14], where the manipulator tracks the aerial robot attitude dynamics during all the translational motion. In [15], the manipulator static effects on the UAV are estimated and compensated through the thrust and torques with a multilayer architecture control. In [16], [17], the problem of disturbance due to the manipulator's presence is handled by adaptation of the control law. When combining a UAV and a robotic manipulator, their dynamics are coupled, and controllers that consider the complete dynamics are found. In [18], cartesian impedance control is studied, while [19] designs a passivity-based controller. Robust and/or adaptive controllers are developed in [20], [21] that control the motion of a multirotor while the manipulator is driven to a desired position carrying a load.

In this work, we also consider the complete quadrotor-manipulator system's dynamics in the control design and analysis. We provide a change of coordinates which splits the system into two decoupled subsystems, one concerning the dynamics of the center of mass of the quadrotor-manipulator system; and another concerning the manipulator's orientation dynamics. These subsystems' dynamics are similar to those of quadrotor's dynamics, and we propose controllers that guarantee that the quadrotor tracks a desired position trajectory, while the manipulator's orientation tracks a desired orientation. Finally, we also consider an input disturbance on the thrust of the quadrotor, and one of our main contributions concerns a disturbance estimate method that guarantees that the previous tracking objectives are still accomplished; and where the disturbance estimate depends

The authors are with the School of Electrical Engineering, KTH Royal Institute of Technology, SE-100 44, Stockholm, Sweden. Email addresses: {ppereira, dimos}@kth.se and zanellar@outlook.com. This work was supported from the EU H2020 Research and Innovation Programme under GA No.644128 (AEROWORKS), the Swedish Research Council (VR), the Swedish Foundation for Strategic Research (SSF) and the KAW Foundation.

on the position tracking error and the orientation tracking error according to different gains, owing to the decoupling. The remainder of this paper is structured as follows. In Section III, we provide a model of the quadrotor-manipulator system, and we describe the tracking problem. In Sections IV and V, we provide control laws that guarantee the tracking objective is accomplished. Finally, in Section VI, simulations and experiments are provided that validate the proposed algorithms.

II. Notation

Given $\Omega_1 \subseteq \mathbb{R}^n$ and $\Omega_2 \subseteq \mathbb{R}^m$, and a function $\mathbf{f} : \Omega_1 \mapsto \Omega_2$, we say $\mathbf{f} \in \mathcal{C}^n(\Omega_1, \Omega_2)$ if all its partial derivatives, up to order n inclusive, are continuous in Ω_1. Moreover, if $\Omega_1 = \mathbb{R}_{\geq 0}$, we denote $\mathbf{f} \in \mathcal{C}^n(\Omega_2)$ for brevity. Given $f \in \mathcal{C}^n(\Omega_2)$, we denote $f^{(i)}(t) := \frac{d^i f(t)}{dt^i}$ for all $t \geq 0$ and $i \in \{0, \cdots, n\}$. Consider a system with state $\mathbf{x} \in \mathcal{C}(\Omega_{\mathbf{x}} \subseteq \mathbb{R}^n)$, a control input $\mathbf{u}_{\mathbf{x}} \in \mathcal{C}(\mathcal{U}_{\mathbf{x}} \subseteq \mathbb{R}^m)$, and denote $\Delta_{\mathbf{x}} \subseteq \mathbb{R}_{\geq 0} \times \Omega_{\mathbf{x}}$. We denote by $\mathbf{f}_{\mathbf{x}} \in \mathcal{C}(\Delta_{\mathbf{x}} \times \mathbb{R}^m, \mathbb{R}^n)$ the open loop vector field, i.e., given $\mathbf{u}_{\mathbf{x}} \in \mathcal{C}(\mathcal{U}_{\mathbf{x}})$, $\dot{\mathbf{x}}(t) = \mathbf{f}_{\mathbf{x}}(t, \mathbf{x}(t), \mathbf{u}_{\mathbf{x}}(t))$. Given a control law $\mathbf{u}_{\mathbf{x}}^{cl} \in \mathcal{C}(\Delta_{\mathbf{x}}, \mathcal{U}_{\mathbf{x}})$, we denote by $\mathbf{f}_{\mathbf{x}}^{cl}(t, \mathbf{x}) := \mathbf{f}_{\mathbf{x}}(t, \mathbf{x}, \mathbf{u}_{\mathbf{x}}^{cl}(t, \mathbf{x}))$ the closed-loop vector field. Moreover, given $V_{\mathbf{x}} \in \mathcal{C}^1(\Delta_{\mathbf{x}}, \mathbb{R}_{\geq 0})$, we denote $W_{\mathbf{x}}(t, \mathbf{x}) := -\frac{\partial V_{\mathbf{x}}(t,\mathbf{x})}{\partial t} - \frac{\partial V_{\mathbf{x}}(t,\mathbf{x})}{\partial \mathbf{x}}^T \mathbf{f}_{\mathbf{x}}^{cl}(t, \mathbf{x})$. Finally, we say $\mathbf{x}^\star \in \mathcal{C}^1(\Omega_{\mathbf{x}})$ is an equilibrium trajectory of $\dot{\mathbf{x}}(t) = \mathbf{f}_{\mathbf{x}}^{cl}(t, \mathbf{x}(t))$ if $\dot{\mathbf{x}}^\star(t) = \mathbf{f}_{\mathbf{x}}^{cl}(t, \mathbf{x}^\star(t))$ and if $\mathbf{0}$ is an equilibrium of $\dot{\mathbf{e}}(t) = \mathbf{f}_{\mathbf{e}}^{cl}(t, \mathbf{e}(t))$, where $\mathbf{e}(t) = \mathbf{x}(t) - \mathbf{x}^\star(t)$ and $\mathbf{f}_{\mathbf{e}}^{cl}(t, \mathbf{e}) := \mathbf{f}_{\mathbf{x}}^{cl}(t, \mathbf{e} + \mathbf{x}^\star(t)) - \dot{\mathbf{x}}^\star(t)$. Given an equilibrium trajectory $\mathbf{x}^\star(\cdot)$, we denote by $\mathbf{u}_{\mathbf{x}}^{cl,\star}(\cdot) := \mathbf{u}_{\mathbf{x}}^{cl}(\cdot, \mathbf{x}^\star(\cdot))$ the equilibrium control input. We denote by $\mathbf{e}_i$ the i^{th} canonical basis vector of $\mathbb{R}^n$; and by $\mathcal{S} : \mathbb{R}^3 \mapsto \mathbb{R}^{3\times 3}$ the skew symmetric matrix satisfying $\mathcal{S}(\mathbf{a})\mathbf{b} = \mathbf{a} \times \mathbf{b}$ for any $\mathbf{a}, \mathbf{b} \in \mathbb{R}^3$.

III. Modeling

Consider a quadrotor vehicle and a point mass load attached to each other by a rigid manipulator, as illustrated in Fig. 1. The manipulator end-points coincide with the quadrotor's and the load's center of mass. Moreover, we assume there is a ball joint connecting the quadrotor's center of mass and one of the manipulator's end-point, which overlap; and finally we assume that an input torque on the manipulator is available. Under the absence of such an input torque, the load attached to one of the manipulator's end-point behaves as a slung load, that can swing with respect to the quadrotor. When the ball joint is locked, the input torque is determined from this constraint, and the manipulator moves rigidly with the quadrotor. Also, notice that the manipulator imposes a kinematic constraint on the system, namely it enforces the distance between the quadrotor's and load's positions to be constant and equal to the manipulator's length, which we assume is constant. Later, we prove the quadrotor-manipulator system is differentially flat with respect to the system's center of mass and the manipulator's orientation. With that in mind, the focus of this paper is on providing closed-loop control laws that guarantee that the system's center of mass follows a desired trajectory and that the manipulator's orientation follows a desired orientation.

We denote by $\mathbf{P} \in \mathcal{C}(\mathbb{R}^3)$ and $\mathbf{p} \in \mathcal{C}(\mathbb{R}^3)$ the quadrotor's and the load's center of mass positions, respectively; by $\mathbf{V} \in \mathcal{C}(\mathbb{R}^3)$ and $\mathbf{v} \in \mathcal{C}(\mathbb{R}^3)$ the quadrotor's and the load's center of mass velocities; and by $M > 0$ and $m > 0$ the quadrotor's and load's masses, respectively. We denote by $\mathbf{n} \in \mathcal{C}(\mathcal{S}^2)$ the manipulator's unit vector, pointing from the load to the quadrotor; by $T \in \mathcal{C}(\mathbb{R})$ the tension/compression on the manipulator; by $L \in \mathbb{R}_{>0}$ the manipulator's length; and by $\boldsymbol{\tau} \in \mathcal{C}(\mathbb{R}^3)$ the torque acting on the manipulator – later, we constraint this torque to be orthogonal to the manipulator's unit vector, which implies that the torque does not drive the manipulator to rotate around itself. For brevity, and hereafter, the force acting along the manipulator's orientation is denoted by tension; however, we emphasize that the manipulator is rigid, and it can withstand compressive forces, which are thus represented by negatives tensions. Finally, we denote by $U \in \mathcal{C}(\mathbb{R})$ the quadrotor's thrust; by $\mathcal{R} \in \mathcal{C}(\mathcal{SO}(3))$ the quadrotor's rotation matrix, with $\mathbf{r} := \mathcal{R}\mathbf{e}_3 \in \mathcal{C}(\mathcal{S}^2)$ being the quadrotor's direction where input thrust is provided; and by $\boldsymbol{\varpi} \in \mathcal{C}(\mathbb{R}^3)$ the quadrotor's angular velocity expressed in the inertial reference frame. We assume $U \in \mathcal{C}(\mathbb{R})$ and $\boldsymbol{\varpi} \in \mathcal{C}(\mathbb{R}^3)$ are inputs to the quadrotor-manipulator system.

Denote by $[\mathbf{p}^T\, \mathbf{v}^T\, \mathbf{P}^T\, \mathbf{V}^T \mathbf{r}^T] =: \mathbf{z} \in \mathcal{C}(\Omega_{\mathbf{z}})$ the state of the quadrotor-load system, where $\Omega_{\mathbf{z}} = \{\mathbf{z} \in \mathbb{R}^{12} \times \mathcal{S}^2 : \|\mathbf{P} - \mathbf{p}\| = L, (\mathbf{V}-\mathbf{v})^T(\mathbf{P}-\mathbf{p}) = 0\}$; and by $\mathcal{U}_{\mathbf{z}} := [U\, \boldsymbol{\varpi}^T \boldsymbol{\tau}^T]^T \in \mathcal{C}(\mathcal{U}_{\mathbf{z}} := \mathbb{R}\times\mathbb{R}^3\times\mathbb{R}^3)$ the control input. The state $\mathbf{z}(\cdot)$ evolves according to the dynamics

$$\dot{\mathbf{z}}(t) = \mathbf{f}_{\mathbf{z}}(\mathbf{z}(t), \mathbf{u}_{\mathbf{z}}(t)), \tag{1}$$

where $\mathbf{f}_{\mathbf{z}} \in \mathcal{C}(\Omega_{\mathbf{z}} \times \mathcal{U}_{\mathbf{z}}, \mathbb{R}^{15})$ is defined as

$$\mathbf{f}_{\mathbf{z}}(\mathbf{z}, \mathbf{u}_{\mathbf{z}}) = \begin{bmatrix} \mathbf{v} \\ \frac{\bar{T}(\mathbf{z}, \mathbf{u}_{\mathbf{z}} + b\mathbf{e}_1)}{m} \bar{\mathbf{n}}(\mathbf{z}) + \mathcal{S}\left(\bar{\mathbf{n}}(\mathbf{z})\right) \frac{\boldsymbol{\tau}}{mL} - g\mathbf{e}_3 \\ \mathbf{V} \\ \frac{U+b}{M}\mathbf{r} - \frac{\bar{T}(\mathbf{z}, \mathbf{u}_{\mathbf{z}} + b\mathbf{e}_1)}{M} \bar{\mathbf{n}}(\mathbf{z}) - \mathcal{S}\left(\bar{\mathbf{n}}(\mathbf{z})\right) \frac{\boldsymbol{\tau}}{ML} - g\mathbf{e}_3 \\ \mathcal{S}\left(\boldsymbol{\varpi}\right) \mathbf{n} \end{bmatrix} \tag{2}$$

where g is the acceleration due to gravity, and where $\bar{\mathbf{n}} : \Omega_{\mathbf{z}} \mapsto \mathcal{S}^2$ and $\bar{T} : \Omega_{\mathbf{z}} \times \mathcal{U}_{\mathbf{z}} \mapsto \mathbb{R}$ are defined as

$$\bar{\mathbf{n}}(\mathbf{z}) = \frac{\mathbf{P} - \mathbf{p}}{\|\mathbf{P} - \mathbf{p}\|} = \frac{\mathbf{P} - \mathbf{p}}{L} \tag{3}$$

$$\bar{T}(\mathbf{z}, \mathbf{u}_{\mathbf{z}}) = \frac{m}{M+m}\left(U\mathbf{r}^T\bar{\mathbf{n}}(\mathbf{z}) + \frac{M}{L}\|\mathbf{V} - \mathbf{v}\|^2\right), \tag{4}$$

and where $b \in \mathbb{R}$ is a constant unknown disturbance acting on the thrust input (and $\mathbf{e}_1 \in \mathbb{R}^7$). The function $\bar{\mathbf{n}}(\cdot)$ in (3) is related with the manipulator's orientation, while the function $\bar{T}(\cdot, \cdot)$ in (4) is related with the tension exerted on the manipulator; i.e., given $\mathbf{u}_z \in \mathcal{C}(\mathcal{U}_{\mathbf{z}})$ and along a solution $\mathbf{z}(\cdot)$ of (1), it follows that $\mathbf{n}(t) = \bar{\mathbf{n}}(\mathbf{z}(t))$ and that $T(t) = \bar{T}(\mathbf{z}(t), \mathbf{u}_z(t) + b\mathbf{e}_1)$, for all $t \geq 0$. Let us provide some insight on how the vector field (2) is derived. One alternative is by means of the Euler-Lagrange formalism. Here we pursue a different approach. Firstly, and with the help of Fig. 1, Newton's second law for the centers of mass of the quadrotor and the load yield the equations in (2), except for $\bar{\mathbf{n}}(\cdot)$ and $\bar{T}(\cdot, \cdot)$ in (3) and (4), respectively. For

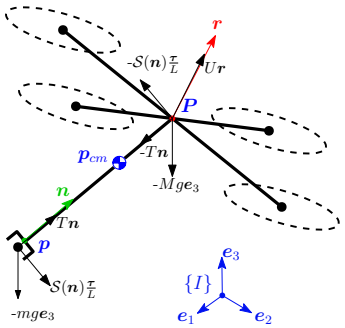

Fig. 1: Modeling of quadrotor-manipulator system

the latter, the manipulator imposes a kinematic constraint, namely $\|\mathbf{P}(t)-\mathbf{p}(t)\| = L\ \forall t \geq 0$, which leads to (3) and (4) by time differentiation. Indeed, differentiating once with respect to time yields $\frac{\mathbf{P}^T(\cdot)-\mathbf{p}^T(\cdot)}{\|\mathbf{P}(\cdot)-\mathbf{p}(\cdot)\|}(\mathbf{V}(\cdot)-\mathbf{v}(\cdot)) = \mathbf{n}^T(\cdot)(\mathbf{V}(\cdot)-\mathbf{v}(\cdot)) = 0$, i.e., $\mathbf{V}(\cdot)-\mathbf{v}(\cdot)$ is always orthogonal to the manipulator's unit vector $\mathbf{n}(\cdot)$. On the other hand, differentiating twice with respect to time yields

$$\begin{aligned}&\mathbf{n}^T(\cdot)(\ddot{\mathbf{P}}(\cdot)-\ddot{\mathbf{p}}(\cdot))+\tfrac{\|\mathbf{V}(\cdot)-\mathbf{v}(\cdot)\|^2}{L}=0 \Leftrightarrow\\ \Leftrightarrow &T(\cdot)=\tfrac{m}{M+m}\left((U(\cdot)+b)\mathbf{r}(\cdot)\mathbf{n}^T(\cdot)+\tfrac{M}{L}\|\mathbf{V}(\cdot)-\mathbf{v}(\cdot)\|^2\right).\end{aligned} \quad (5)$$

It is now obvious that $T(\cdot)=\bar{T}(\mathbf{z}(\cdot),\mathbf{u}_z(\cdot)+b\mathbf{e}_1)$, with $T(\cdot)$ in (5) and $\bar{T}(\cdot,\cdot)$ in (4). Moreover, notice that $\Omega_{\mathbf{z}}=\{\mathbf{z}\in\mathbb{R}^{12}\times\mathcal{S}^2 : \|\mathbf{P}-\mathbf{p}\|=L, (\mathbf{V}-\mathbf{v})^T(\mathbf{P}-\mathbf{p})=0\}$ is in fact positively invariant, i.e., the tension in the manipulator guarantees that the distance between the quadrotor's and the load's center of mass remains constant and equal to the manipulator length. Notice also that the tension on the manipulator does not depend on the torque input, since this torque does not attempt to drive the quadrotor away from the load; rather it only attempts to make the quadrotor and load rotate around each other.

Problem III.1: Given the system (1), a desired trajectory $\mathbf{P}^\star : \mathbb{R}_{\geq 0}\mapsto\mathbb{R}^3$ and a desired orientation $\mathbf{n}^\star : \mathbb{R}_{\geq 0}\mapsto\mathcal{S}^2$, design $U : \mathbb{R}_{\geq 0}\mapsto\mathbb{R}$, $\boldsymbol{\varpi} : \mathbb{R}_{\geq 0}\mapsto\mathbb{R}^3$ and $\boldsymbol{\tau} : \mathbb{R}_{\geq 0}\mapsto\mathbb{R}^3$, such that $\lim_{t\to\infty}(\mathbf{P}(t)-\mathbf{P}^\star(t))=\mathbf{0}$ and $\lim_{t\to\infty}(\mathbf{n}(t)-\mathbf{n}^\star(t))=\mathbf{0}$.

Problem III.1 can be restated as finding a control law for $\mathbf{u}_{\mathbf{z}}(\cdot)$, such that the quadrotor follows a desired trajectory, while the manipulator follows a desired orientation. For example, we may want the quadrotor to describe a circular motion, while the manipulator is always pointing downwards. As shall be seen later, Problem III.1 can also be restated as finding a control law for $\mathbf{u}_{\mathbf{z}}(\cdot)$, such that the center of mass of the quadrotor-manipulator system follows a desired trajectory given by $\mathbf{P}^\star(\cdot)-L\frac{m}{M+m}\mathbf{n}^\star(\cdot)$, while the manipulator follows the desired orientation given by $\mathbf{n}^\star(\cdot)$.

IV. Control Strategy

In this section, we provide a control law that guarantees that the goal stated in Problem III.1 is accomplished. First, we provide a smooth coordinate transformation that simplifies the control design, and which has a physical interpretation. Secondly, we discuss some differential flatness properties that the system (1) exhibits, and which also provides further physical insight into the problem. Finally, we describe the proposed control law and provide results that guarantee that the goal as stated in Problem III.1 is achieved.

A. Coordinate transformation

In this subsection, we provide a coordinate transformation between the state as defined in Section III and a new state. This transformation will prove useful in the control design, and moreover, for the transformed state, we will be able to decouple the control of some of the state components. First, denote $\mathbf{p}_{cm}\in\mathcal{C}(\Omega_{\mathbf{z}},\mathbb{R}^3)$ and $\mathbf{v}_{cm}\in\mathcal{C}(\Omega_{\mathbf{z}},\mathbb{R}^3)$ defined as

$$\mathbf{p}_{cm}(\mathbf{z})=\frac{M\mathbf{P}+m\mathbf{p}}{M+m}, \mathbf{v}_{cm}(\mathbf{z})=\frac{M\mathbf{V}+m\mathbf{v}}{M+m}, \quad (6)$$

where, physically, $\mathbf{p}_{cm}(\mathbf{z})$ and $\mathbf{v}_{cm}(\mathbf{z})$ stand, respectively, for the position and velocity of the center of mass of the quadrotor-manipulator system with state $\mathbf{z}\in\Omega_{\mathbf{z}}$ (see Fig. 1). It follows (6) and (3), that

$$\mathbf{P}=\mathbf{p}_{cm}(\mathbf{z})+\bar{\mathbf{n}}(\mathbf{z})\tfrac{Lm}{M+m}\Leftrightarrow\mathbf{p}_{cm}(\mathbf{z})=\mathbf{P}-\tfrac{Lm}{M+m}\bar{\mathbf{n}}(\mathbf{z}), \quad (7)$$

$$\mathbf{p}=\mathbf{p}_{cm}(\mathbf{z})-\bar{\mathbf{n}}(\mathbf{z})\tfrac{LM}{M+m}\Leftrightarrow\mathbf{p}_{cm}(\mathbf{z})=\mathbf{p}+\tfrac{Lm}{M+m}\bar{\mathbf{n}}(\mathbf{z}). \quad (8)$$

Equation (7) motivates the definition $\mathbf{p}^\star_{cm}(t) := \mathbf{P}^\star(t)-\frac{Lm}{M+m}\mathbf{n}^\star(t)$ as the desired trajectory for the system's center of mass. Consider now the manipulator's unit vector defined in (3), and the function $\bar{\boldsymbol{\omega}}\in\mathcal{C}(\Omega_{\mathbf{z}},\mathbb{R}^3)$ defined as $\bar{\boldsymbol{\omega}}(\mathbf{z})=\mathcal{S}(\bar{\mathbf{n}}(\mathbf{z}))\frac{\mathbf{V}-\mathbf{v}}{L}$, where, physically, $\bar{\mathbf{n}}(\mathbf{z})$ and $\bar{\boldsymbol{\omega}}(\mathbf{z})$ stand, respectively, for the manipulator's orientation and angular velocity of the quadrotor-manipulator system with state $\mathbf{z}\in\Omega_{\mathbf{z}}$. For convenience, denote

$$\mathbf{x}^T := [\mathbf{x}_1^T\ \mathbf{x}_2^T] := [[\mathbf{e}^T\ \boldsymbol{\upsilon}^T\ \mathbf{r}^T]\ [\mathbf{n}^T\ \boldsymbol{\omega}^T]]\in\mathcal{C}(\Omega_{\mathbf{x}}) \quad (9)$$

where $\Omega_{\mathbf{x}}=\mathbb{R}^3\times\mathbb{R}^3\times\mathcal{S}^2\times\mathcal{S}^2\times\mathbb{R}^3$, and consider, for each positive time instant t, the diffeomorphism $T^{\mathbf{x}}_{\mathbf{z}}(t,\cdot)\in\mathcal{C}^1(\Omega_{\mathbf{z}},\Omega_{\mathbf{x}})$ – where, for brevity, we denote $T^{\mathbf{z}}_{\mathbf{x}}(\cdot,\mathbf{x}) := (T^{\mathbf{x}}_{\mathbf{z}})^{-1}(\cdot,\mathbf{x})$ – defined as

$$T^{\mathbf{x}}_{\mathbf{z}}(t,\mathbf{z})=\begin{bmatrix}\mathbf{p}_{cm}(\mathbf{z})-\mathbf{p}^{\star(0)}_{cm}(t)\\ \mathbf{v}_{cm}(\mathbf{z})-\mathbf{p}^{\star(1)}_{cm}(t)\\ \mathbf{r}\\ \bar{\mathbf{n}}(\mathbf{z})\\ \bar{\boldsymbol{\omega}}(\mathbf{z})\end{bmatrix}, T^{\mathbf{z}}_{\mathbf{x}}(t,\mathbf{x})=\begin{bmatrix}\mathbf{e}+\mathbf{p}^{\star(0)}_{cm}(t)-\mathbf{n}\frac{M}{M+m}\\ \boldsymbol{\upsilon}+\mathbf{p}^{\star(1)}_{cm}(t)-\mathcal{S}(\boldsymbol{\omega})\mathbf{n}\frac{M}{M+m}\\ \mathbf{e}+\mathbf{p}^{\star(0)}_{cm}(t)+\mathbf{n}\frac{m}{M+m}\\ \boldsymbol{\upsilon}+\mathbf{p}^{\star(1)}_{cm}(t)+\mathcal{S}(\boldsymbol{\omega})\mathbf{n}\frac{m}{M+m}\\ \mathbf{r}\end{bmatrix} \quad (10)$$

Later, we consider, for each positive time instant t, the state $\mathbf{x}(t)=T^{\mathbf{x}}_{\mathbf{z}}(t,\mathbf{z}(t))$ (see (9)), which means $\mathbf{e}(t)$ corresponds to the position tracking error of the center of mass; $\boldsymbol{\upsilon}(t)$ corresponds to the velocity tracking error of the center of mass; $\mathbf{r}(t)$ corresponds to the quadrotor's direction where thrust is provided; $\mathbf{n}(t)$ corresponds to the manipulator's orientation; and $\boldsymbol{\omega}(t)$ corresponds to the manipulator's angular velocity. Finally, denote $\mathbf{u}_{\mathbf{x}}^T := [\mathbf{u}_{\mathbf{x}_1}^T\ \mathbf{u}_{\mathbf{x}_2}^T] := [[u\ \boldsymbol{\varpi}^T]\ \boldsymbol{\alpha}^T]\in\mathcal{C}(\mathcal{U}_{\mathbf{x}} := \mathbb{R}^7)$, and consider the functions $T^{\mathbf{u}_{\mathbf{z}}}_{\mathbf{u}_{\mathbf{x}}}\in\mathcal{C}(\Omega_{\mathbf{x}}\times\mathcal{U}_{\mathbf{x}},\mathcal{U}_{\mathbf{z}})$ and $T^{\mathbf{u}_{\mathbf{x}}}_{\mathbf{u}_{\mathbf{z}}}\in\mathcal{C}(\Omega_{\mathbf{z}}\times\mathcal{U}_{\mathbf{z}},\mathcal{U}_{\mathbf{x}})$ defined as

$$T^{\mathbf{u}_{\mathbf{z}}}_{\mathbf{u}_{\mathbf{x}}}(\mathbf{x},\mathbf{u}_{\mathbf{x}})=\begin{bmatrix}(M+m)u\\ \boldsymbol{\varpi}\\ L^2\frac{Mm}{M+m}\mathcal{S}(\mathbf{n})\left(\boldsymbol{\alpha}-\frac{(M+m)u}{LM}\mathbf{r}\right)\end{bmatrix}, \quad (11)$$

and

$$T^{\mathbf{u}_{\mathbf{x}}}_{\mathbf{u}_{\mathbf{z}}}(\mathbf{z},\mathbf{u}_{\mathbf{z}})=\begin{bmatrix}\frac{U}{M+m}\\ \boldsymbol{\varpi}\\ -\frac{1}{LM}\mathcal{S}(\bar{\mathbf{n}}(\mathbf{z}))\left(\frac{M+m}{m}\frac{\boldsymbol{\tau}}{L}+U\mathcal{S}(\bar{\mathbf{n}}(\mathbf{z}))\mathbf{r}\right)\end{bmatrix} \quad (12)$$

which provide input transformations that will become clear later in this section. In particular, we emphasize that $\mathbf{u}_{\mathbf{z}}=T^{\mathbf{u}_{\mathbf{z}}}_{\mathbf{u}_{\mathbf{x}}}(T^{\mathbf{x}}_{\mathbf{z}}(t,\mathbf{z}),T^{\mathbf{u}_{\mathbf{x}}}_{\mathbf{u}_{\mathbf{z}}}(\mathbf{z},\mathbf{u}_{\mathbf{z}})))$ for all $t\geq 0$ and for all $(\mathbf{z},\mathbf{u}_{\mathbf{z}})\in$

$\{(\mathbf{z},\mathbf{u}_\mathbf{z}) \in \Omega_\mathbf{z} \times \mathcal{U}_\mathbf{z} : \boldsymbol{\tau}^T \bar{\mathbf{n}}(\mathbf{z}) = 0\}$; and that $\mathbf{u}_\mathbf{x} = T^{\mathbf{u}_\mathbf{x}}_{\mathbf{u}_\mathbf{z}}(T^\mathbf{z}_\mathbf{x}(t,\mathbf{x}), T^{\mathbf{u}_\mathbf{z}}_{\mathbf{u}_\mathbf{x}}(\mathbf{x},\mathbf{u}_\mathbf{x}))$ for all $t \geq 0$ and for all $(\mathbf{x},\mathbf{u}_\mathbf{x}) \in \{(\mathbf{x},\mathbf{u}_\mathbf{x}) \in \Omega_\mathbf{x} \times \mathcal{U}_\mathbf{x} : \boldsymbol{\alpha}^T \mathbf{n} = 0\}$.

Consider then a trajectory $\mathbf{z}(\cdot)$ of (1), the mapping (10), and $\mathbf{x}(\cdot) = T^\mathbf{x}_\mathbf{z}(\cdot, \mathbf{z}(\cdot))$. It follows from (1), that $\dot{\mathbf{x}}(t) = \mathbf{f}_\mathbf{x}(t,\mathbf{x}(t),\mathbf{u}_\mathbf{x}(t))$ where

$$\begin{aligned}\mathbf{f}_\mathbf{x}(t,\mathbf{x},\mathbf{u}_\mathbf{x}) &= \left(\tfrac{\partial T^\mathbf{x}_\mathbf{z}(t,\mathbf{z})}{\partial t} + \tfrac{\partial T^\mathbf{x}_\mathbf{z}(t,\mathbf{z})}{\partial \mathbf{z}}^T \mathbf{f}_\mathbf{z}(\mathbf{z},\mathbf{u}_\mathbf{z})\right)\Big|_{\substack{\mathbf{z}=T^\mathbf{z}_\mathbf{x}(t,\mathbf{x}) \\ \mathbf{u}_\mathbf{z}=T^{\mathbf{u}_\mathbf{z}}_{\mathbf{u}_\mathbf{x}}(\mathbf{x},\mathbf{u}_\mathbf{x})}} \\ &= \begin{bmatrix} \boldsymbol{v} \\ u\mathbf{r} - (g\mathbf{e}_3 + \mathbf{p}^{\star(2)}_{cm}(t)) \\ \mathcal{S}(\boldsymbol{\varpi})\,\mathbf{r} \\ \mathcal{S}(\boldsymbol{\omega})\,\mathbf{n} \\ \mathcal{S}(\mathbf{n})\,\boldsymbol{\alpha} \end{bmatrix} + \begin{bmatrix} \mathbf{0} \\ \frac{\mathbf{r}}{M+m} \\ \mathbf{0} \\ \mathbf{0} \\ \mathcal{S}(\mathbf{n})\,\frac{\mathbf{r}}{LM} \end{bmatrix} b \\ &=: \begin{bmatrix} \mathbf{f}_{\mathbf{x}_1}(t,\mathbf{x}_1,\mathbf{u}_{\mathbf{x}_1}) \\ \mathbf{f}_{\mathbf{x}_2}(\mathbf{x}_2,\mathbf{u}_{\mathbf{x}_2}) \end{bmatrix} + \Phi(\mathbf{x})b. \end{aligned} \tag{13}$$

Attaining (13) follows from straightforward but lengthy computations, and those details are omitted here due to paper length constraints. Notice now that the coordinate change in (10) and the input change in (11) lead to a vector field (13), where the open-loop dynamics of the states $\mathbf{x}_1$ and $\mathbf{x}_2$ (see (9)) are not coupled. In fact, in the absence of a disturbance, i.e., if $b = 0$, we can design control laws for $\mathbf{u}_{\mathbf{x}_1}$ and $\mathbf{u}_{\mathbf{x}_2}$ that depend only on the respective states.

B. Differential Flatness

In this subsection, we show that the system with vector field (13) is differentially flat with respect to the output $\mathbf{y}(t) = [\mathbf{y}_1^T(t)\,\mathbf{y}_2^T(t)]^T = [\mathbf{e}^T(t)\,\mathbf{n}^T(t)]^T$. In fact, it is easy to verify that given

$$\begin{aligned}
&\tilde{\mathbf{x}}_1(t,\mathbf{y}_1^{(0)},\mathbf{y}_1^{(1)},\mathbf{y}_1^{(2)}) = \begin{bmatrix}\mathbf{y}_1^{(0)T} & \mathbf{y}_1^{(1)T} & \frac{g\mathbf{e}_3+\mathbf{p}^{\star(2)}_{cm}(t)-\mathbf{y}_1^{(2)}}{\|g\mathbf{e}_3+\mathbf{p}^{\star(2)}_{cm}(t)-\mathbf{y}_1^{(2)}\|}^T\end{bmatrix}^T, \\
&\tilde{\mathbf{u}}_{\mathbf{x}_1}(t,\mathbf{y}_1^{(0)},\mathbf{y}_1^{(1)},\mathbf{y}_1^{(2)},\mathbf{y}_1^{(3)}) = \begin{bmatrix} \|g\mathbf{e}_3+\mathbf{p}^{\star(2)}_{cm}(t)-\mathbf{y}_1^{(2)}\| - \frac{b}{M+m} \\ \mathcal{S}\left(\frac{g\mathbf{e}_3+\mathbf{p}^{\star(2)}_{cm}(t)-\mathbf{y}_1^{(2)}}{\|g\mathbf{e}_3+\mathbf{p}^{\star(2)}_{cm}(t)-\mathbf{y}_1^{(2)}\|}\right)\frac{\mathbf{p}^{\star(3)}_{cm}(t)-\mathbf{y}_1^{(3)}}{\|g\mathbf{e}_3+\mathbf{p}^{\star(2)}_{cm}(t)\|}\end{bmatrix}, \\
&\tilde{\mathbf{x}}_2(\mathbf{y}_2^{(0)},\mathbf{y}_2^{(1)}) = \begin{bmatrix}\mathbf{y}_2^{(0)} \\ \mathcal{S}(\mathbf{y}_2^{(0)})\,\mathbf{y}_2^{(1)}\end{bmatrix}, \tilde{\mathbf{u}}_{\mathbf{x}_2}(\mathbf{y}_1^{(2)}) = \mathbf{y}_2^{(2)} - \tfrac{b}{LM},
\end{aligned}$$

it follows that, for $\tilde{\mathbf{x}} = [\tilde{\mathbf{x}}_1^T\,\tilde{\mathbf{x}}_2^T]^T$ and $\tilde{\mathbf{u}}_\mathbf{x} = [\tilde{\mathbf{u}}_{\mathbf{x}_1}^T\,\tilde{\mathbf{u}}_{\mathbf{x}_2}^T]^T$, $\dot{\tilde{\mathbf{x}}} = \mathbf{f}_\mathbf{x}(t,\tilde{\mathbf{x}},\tilde{\mathbf{u}}_\mathbf{x})$. As such, the system with vector field (2) is differentially flat with respect to the output $\mathbf{y}(t) = [\mathbf{e}^T(t)\,\mathbf{n}(t)]^T \overset{(10)}{=} [(\mathbf{p}_{cm}(\mathbf{z}(t)) - \mathbf{p}^\star_{cm}(t))^T\ \bar{\mathbf{n}}(\mathbf{z}(t))^T]^T$, i.e., it is differentially flat with respect to the center of mass position and the manipulator's orientation. Physically, it implies that the motion described by the quadrotor-manipulator system's center of mass, and the motion described by the manipulator's orientation completely determine the system's state. Also, it follows from (7) and (8) that the system with vector field (2) is also differentially flat with respect to the quadrotor's position and the manipulator orientation – since these two dictate the center of mass position; and it is also differentially flat with respect to the load's position and the manipulator orientation – since these two also dictate the center of mass position.

C. Disturbance Removal

In this section, we provide a solution that accomplishes the goal described in Problem III.1, when a constant unknown disturbance $b \in \{\beta \in \mathbb{R}^3 : |\beta| \leq b^{\max}\} =: \Omega_b$ exists, for some known $b^{\max} \geq 0$. Denote $\hat{b} \in \mathcal{C}(\mathbb{R})$ as a disturbance estimate whose dynamics we design next such that the goal described in Problem III.1 is accomplished. For convenience, and since the disturbance estimate is dynamic, denote $\tilde{\mathbf{x}} = [\mathbf{x}^T\,\hat{b}]^T \in \mathcal{C}(\Omega_\mathbf{x} \times \mathbb{R} =: \Omega_{\tilde{\mathbf{x}}})$ as an extended state. Also, $\dot{\hat{b}}(t) = f_{\hat{b}}(t,\tilde{\mathbf{x}}(t))$, where $f_{\hat{b}} \in \mathcal{C}(\mathbb{R}_{\geq 0} \times \Omega_{\tilde{\mathbf{x}}}, \mathbb{R})$ is a vector field that is constructed later in this section. As such, it follows that $\dot{\tilde{\mathbf{x}}}(t) = \mathbf{f}_{\tilde{\mathbf{x}}}(t,\tilde{\mathbf{x}}(t),\mathbf{u}_{\tilde{\mathbf{x}}}(t))$, where (note that $\mathbf{u}_{\tilde{\mathbf{x}}} = \mathbf{u}_\mathbf{x}$)

$$\mathbf{f}_{\tilde{\mathbf{x}}}(t,\tilde{\mathbf{x}},\mathbf{u}_{\tilde{\mathbf{x}}}) = \left[\begin{bmatrix} \mathbf{f}_{\mathbf{x}_1}(t,\mathbf{x}_1,\mathbf{u}_{\mathbf{x}_1}) \\ \mathbf{f}_{\mathbf{x}_2}(\mathbf{x}_2,\mathbf{u}_{\mathbf{x}_2}) \end{bmatrix} + \Phi(\mathbf{x})b \right],$$

and moreover (recall, from (11) and (12), that $\mathbf{u}_\mathbf{x} = T^{\mathbf{u}_\mathbf{x}}_{\mathbf{u}_\mathbf{z}}(T^\mathbf{z}_\mathbf{x}(t,\mathbf{x}), T^{\mathbf{u}_\mathbf{z}}_{\mathbf{u}_\mathbf{x}}(\mathbf{x},\mathbf{u}_\mathbf{x})))$

$$\begin{aligned}&\mathbf{f}_{\tilde{\mathbf{x}}}(t,\tilde{\mathbf{x}},T^{\mathbf{u}_\mathbf{x}}_{\mathbf{u}_\mathbf{z}}(T^\mathbf{z}_\mathbf{x}(t,\mathbf{x}),T^{\mathbf{u}_\mathbf{z}}_{\mathbf{u}_\mathbf{x}}(\mathbf{x},\mathbf{u}_\mathbf{x}) - \hat{b}\mathbf{e}_1)) = \\ &= \left[\begin{bmatrix} \mathbf{f}_{\mathbf{x}_1}(t,\mathbf{x}_1,\mathbf{u}_{\mathbf{x}_1}) \\ \mathbf{f}_{\mathbf{x}_2}(\mathbf{x}_2,\mathbf{u}_{\mathbf{x}_2}) \end{bmatrix} + \Phi(\mathbf{x})(b-\hat{b}) \right].\end{aligned} \tag{14}$$

Assumption IV.1: Assume the following functions are available: control laws $\mathbf{u}^{cl}_{\mathbf{x}_1} \in \mathcal{C}(\mathbb{R}_{\geq 0} \times \Omega_{\mathbf{x}_1}, \mathbb{R}^4)$ and $\mathbf{u}^{cl}_{\mathbf{x}_2} \in \mathcal{C}(\mathbb{R}_{\geq 0} \times \Omega_{\mathbf{x}_2}, \mathbb{R}^3)$; Lyapunov functions $V_{\mathbf{x}_1} \in \mathcal{C}^1(\mathbb{R}_{\geq 0} \times \Omega_{\mathbf{x}_1}, \mathbb{R}_{\geq 0})$ and $V_{\mathbf{x}_2} \in \mathcal{C}^1(\mathbb{R}_{\geq 0} \times \Omega_{\mathbf{x}_2}, \mathbb{R}_{\geq 0})$; and functions $W_{\mathbf{x}_1} \in \mathcal{C}^1(\mathbb{R}_{\geq 0} \times \Omega_{\mathbf{x}_1}, \mathbb{R}_{\geq 0})$ and $W_{\mathbf{x}_2} \in \mathcal{C}^1(\mathbb{R}_{\geq 0} \times \Omega_{\mathbf{x}_2}, \mathbb{R}_{\geq 0})$; such that it is guaranteed that $\dot{V}_{\mathbf{x}_1}(t,\mathbf{x}_1(t)) = -W_{\mathbf{x}_1}(t,\mathbf{x}_1(t)) \leq 0$ and $\dot{V}_{\mathbf{x}_2}(t,\mathbf{x}_2(t)) = -W_{\mathbf{x}_2}(t,\mathbf{x}_2(t)) \leq 0$, and that $\lim_{t\to\infty} \mathbf{e}(t) = \mathbf{0}$ and that $\lim_{t\to\infty}(\mathbf{n}(t) \pm \mathbf{n}^\star(t)) = \mathbf{0}$, along solutions of $\dot{\mathbf{x}}_1(t) = \mathbf{f}^{cl}_{\mathbf{x}_1}(t,\mathbf{x}_1(t))$ and of $\dot{\mathbf{x}}_2(t) = \mathbf{f}^{cl}_{\mathbf{x}_2}(t,\mathbf{x}_2(t))$. Additionally, $W_{\mathbf{x}_1}(t,\mathbf{x}_1) = 0 \Rightarrow \mathbf{e} = \mathbf{0}$ and $W_{\mathbf{x}_2}(t,\mathbf{x}_2) = 0 \Rightarrow \mathbf{n} = \pm\mathbf{n}^\star(t)$ for all $t \geq 0$; moreover, there exists $\xi > 0$ such that $W_{\mathbf{x}_2}(t,\mathbf{x}_2) = 0 \wedge \mathbf{x}_2 \in \{\mathbf{x}_2 \in \Omega_{\mathbf{x}_2} : V_{\mathbf{x}_2}(t,\mathbf{x}_2) < \xi\} \Rightarrow \mathbf{n} = \mathbf{n}^\star(t)$ for all $t \geq 0$.

Possible control laws $\mathbf{u}^{cl}_{\mathbf{x}_1} \in \mathcal{C}(\mathbb{R}_{\geq 0} \times \Omega_{\mathbf{x}_1}, \mathbb{R}^4)$ and $\mathbf{u}^{cl}_{\mathbf{x}_2} \in \mathcal{C}(\Omega_{\mathbf{x}_2}, \mathbb{R}^3)$, satisfying conditions of Assumption IV.1, are found in Section V. If the disturbance b were known, it would suffice to choose $\hat{b}(0) = b$, and $f_{\hat{b}}(t,\tilde{\mathbf{x}}) = 0$, in order to accomplish the goal in Problem III.1. Since b is unknown, a different strategy is pursed, namely the disturbance estimate is updated with a projector operator that guarantees that the disturbance estimate remains in $\Omega_{\hat{b}} := \{\beta \in \mathbb{R}^3 : |\beta| \leq b^{\max} + \epsilon\} \supset \Omega_b$, where $\epsilon > 0$ is a design parameter that can be chosen as small as desired; and provided that $\hat{b}(0) \in \Omega_{\hat{b}}$, which is satisfied if $\hat{b}(0) = 0$. Consider then the vector field (for brevity, denote $V_\mathbf{x}(t,\mathbf{x}) = k_{\hat{b}_1} V_{\mathbf{x}_1}(t,\mathbf{x}_1) + k_{\hat{b}_2} V_{\mathbf{x}_2}(t,\mathbf{x}_2)$)

$$\begin{aligned}f_{\hat{b}}(t,\tilde{\mathbf{x}}) &= \text{Proj}\left(\Phi^T(\mathbf{x})\tfrac{\partial V_\mathbf{x}(t,\mathbf{x})}{\partial \mathbf{x}}, \hat{b}\right), \\ &= \text{Proj}\left(k_{\hat{b}_1}\tfrac{\mathbf{n}^T}{M+m}\tfrac{\partial V_{\mathbf{x}_1}(t,\mathbf{x}_1)}{\partial \boldsymbol{v}} + k_{\hat{b}_2}\tfrac{\mathbf{n}^T\mathcal{S}(\mathbf{r})}{ML}\tfrac{\partial V_{\mathbf{x}_2}(t,\mathbf{x}_2)}{\partial \boldsymbol{\omega}}, \hat{b}\right),\end{aligned} \tag{15}$$

with $\text{Proj}(\cdot,\cdot)$ as defined in [22], and with $k_{\hat{b}_1}$ and $k_{\hat{b}_2}$ as positive constant gains. Consider the Lyapunov function $V_{\tilde{\mathbf{x}}} \in \mathcal{C}^1(\mathbb{R}_{\geq 0} \times \Omega_{\tilde{\mathbf{x}}}, \mathbb{R}_{\geq 0})$, defined as $V_{\tilde{\mathbf{x}}}(t,\tilde{\mathbf{x}}) = k_{\hat{b}_1} V_{\mathbf{x}_1}(t,\mathbf{x}_1) + k_{\hat{b}_2} V_{\mathbf{x}_2}(t,\mathbf{x}_2) + \frac{(b-\hat{b})}{2}$, for which it follows that (see Assumption IV.1, (14) and (15))

$$\begin{aligned}&W_{\tilde{\mathbf{x}}}(t,\tilde{\mathbf{x}}) = k_{\hat{b}_1} W_{\mathbf{x}_1}(t,\mathbf{x}_1) + k_{\hat{b}_2} W_{\mathbf{x}_2}(t,\mathbf{x}_2) + \\ &(b-\hat{b})\left(f_{\hat{b}}(t,\tilde{\mathbf{x}}) - \Phi^T(\mathbf{x})\frac{\partial V_\mathbf{x}(t,\mathbf{x})}{\partial \mathbf{x}}\right) \geq 0.\end{aligned}$$

Since $V(t,\mathbf{x}^\star(t)) = k_{\hat{b}_1}V_{\mathbf{x}}(t,\mathbf{x}_1^\star(t)) + k_{\hat{b}_2}V_{\mathbf{x}_2}(t,\mathbf{x}_2^\star(t)) = 0\,\forall t \geq 0$ and $V(\cdot,\cdot) \geq 0$, it follows that $\frac{\partial V_{\mathbf{x}}(t,\mathbf{x})}{\partial \mathbf{x}}|_{\mathbf{x}=\mathbf{x}^\star(t)} = 0$ for all $t \geq 0$. As such, $f_{\hat{b}}(t,[\mathbf{x}^{\star,T}(t)\,\hat{b}]^T) = 0$ for all $\hat{b} \in \mathbb{R}$ and $t \geq 0$; also the gain $k_{\hat{b}_1}$ may be interpreted as a weight on the disturbance estimate vector field due to the tracking error of the center of mass – associated to $\mathbf{x}_1$; while the gain $k_{\hat{b}_2}$ may be interpreted as a weight on the disturbance estimate vector field due to the tracking error of the manipulator's orientation – associated to $\mathbf{x}_2$. In particular, the ratio $\frac{k_{\hat{b}_1}}{k_{\hat{b}_2}}$ is important, in the sense that it determines how more/less important the tracking error of the center of mass is in estimating the disturbance than the tracking error of the manipulator's orientation. To summarize, the proposed time-varying control law is $\mathbf{u}_{\mathbf{z}}(t) = \mathbf{u}_{\mathbf{z}}^{cl}(t,\mathbf{z}(t))$, where

$$\mathbf{u}_{\mathbf{z}}^{cl}(t,\mathbf{z}) = T_{\mathbf{u}_{\mathbf{x}}}^{\mathbf{u}_{\mathbf{z}}}(\mathbf{x},\mathbf{u}_{\mathbf{x}}^{cl}(t,\mathbf{x}))|_{\mathbf{x}=T_{\mathbf{z}}^{\mathbf{x}}(t,\mathbf{z})} - \hat{b}(t)\mathbf{e}_1, \quad (16)$$

$$\mathbf{u}_{\mathbf{x}}^{cl}(t,\mathbf{x}) = [\mathbf{u}_{\mathbf{x}_1}^{cl,T}(t,\mathbf{x}_1)\,\mathbf{u}_{\mathbf{x}_2}^{cl,T}(t,\mathbf{x}_2)]^T, \quad (17)$$

$$\dot{\hat{b}}(t) = f_{\hat{b}}(t,\tilde{\mathbf{x}}(t)),\ \hat{b}(0) = 0.$$

Theorem IV.1: Consider the system (1) and the control law $\mathbf{u}_{\mathbf{z}}(t) = \mathbf{u}_{\mathbf{z}}^{cl}(t,\mathbf{z}(t))$, with $\mathbf{u}_{\mathbf{z}}^{cl}(\cdot,\cdot)$ as defined in (16) and with functions as specified in Assumption IV.1. It follows that for all $\mathbf{z}(0) \in \Omega_{\mathbf{z}}$, $\lim_{t\to\infty}(\mathbf{P}(t) - \mathbf{P}^\star(t)) = \mathbf{0}$ and that $\lim_{t\to\infty}(\mathbf{n}(t) \pm \mathbf{n}^\star(t)) = \mathbf{0}$. Moreover, if $\mathbf{z}(0) \in \{\mathbf{z} \in \Omega_{\mathbf{z}} : V_{\tilde{\mathbf{x}}}(t,\tilde{\mathbf{x}}) < k_{\hat{b}_2}\xi, \tilde{\mathbf{x}} = [\mathbf{x}^T\,\hat{b}(0)]^T, \mathbf{x} = T_{\mathbf{z}}^{\mathbf{x}}(0,\mathbf{z})\}$, it follows that $\lim\limits_{t\to\infty}(\mathbf{n}(t) - \mathbf{n}^\star(t)) = \mathbf{0}$.

Proof: Consider a trajectory $\tilde{\mathbf{x}}(\cdot)$ of $\dot{\tilde{\mathbf{x}}}(t) = \mathbf{f}_{\tilde{\mathbf{x}}}(t,\tilde{\mathbf{x}}(t),T_{\mathbf{u}_{\mathbf{z}}}^{\mathbf{u}_{\mathbf{x}}}(T_{\mathbf{x}}^{\mathbf{z}}(t,\mathbf{x}),T_{\mathbf{u}_{\mathbf{x}}}^{\mathbf{u}_{\mathbf{z}}}(\mathbf{x},\mathbf{u}_{\tilde{\mathbf{x}}}^{cl}(t,\tilde{\mathbf{x}}(t))) - \hat{b}\mathbf{e}_1))$, with $\mathbf{u}_{\tilde{\mathbf{x}}}^{cl}(\cdot,\cdot)$ as defined in (17) and with $f_{\hat{b}}(\cdot,\cdot)$ as defined in (15). Since $V_{\tilde{\mathbf{x}}}(\cdot,\cdot) \geq 0$ and $\dot{V}_{\tilde{\mathbf{x}}}(t,\tilde{\mathbf{x}}(t)) \leq -W_{\tilde{\mathbf{x}}}(t,\tilde{\mathbf{x}}(t)) \leq 0$, it follows that $V_{\tilde{\mathbf{x}}}(\cdot,\tilde{\mathbf{x}}(\cdot))$ converges to a constant. Moreover, since $\ddot{V}_{\tilde{\mathbf{x}}}(\cdot,\tilde{\mathbf{x}}(\cdot))$ is bounded, i.e. $\sup_{t\geq 0}|\ddot{V}_{\tilde{\mathbf{x}}}(t,\tilde{\mathbf{x}}(t))| = \sup_{t\geq 0}|\dot{W}_{\tilde{\mathbf{x}}}(t,\tilde{\mathbf{x}}(t))| < \infty$, it follows that $\dot{V}_{\tilde{\mathbf{x}}}(\cdot,\tilde{\mathbf{x}}(\cdot))$ is uniformly continuous. Invoking Barbalat's lemma, it follows that $\lim_{t\to\infty}\dot{V}_{\tilde{\mathbf{x}}}(t,\tilde{\mathbf{x}}(t)) = 0 \Rightarrow \lim_{t\to\infty}W_{\mathbf{x}_1}(t,\mathbf{x}_1(t)) = 0 \wedge \lim_{t\to\infty}W_{\mathbf{x}_2}(t,\mathbf{x}_2(t)) = 0$. This in turn implies that $\lim_{t\to\infty}(\mathbf{P}(t) - \mathbf{P}^\star(t)) = \mathbf{0}$ and that $\lim_{t\to\infty}(\mathbf{n}(t) \pm \mathbf{n}^\star(t)) = \mathbf{0}$. Moreover, if $\mathbf{z}(0) \in \{\mathbf{z} \in \Omega_{\mathbf{z}} : V_{\tilde{\mathbf{x}}}(t,\tilde{\mathbf{x}}) < k_{\hat{b}_2}\xi, \tilde{\mathbf{x}} = [\mathbf{x}^T\,\hat{b}(0)]^T, \mathbf{x} = T_{\mathbf{z}}^{\mathbf{x}}(0,\mathbf{z})\}$, then $k_{\hat{b}_2}V_{\mathbf{x}_2}(t,\mathbf{x}_2(t)) \leq V_{\tilde{\mathbf{x}}}(0,\tilde{\mathbf{x}}(0)) < k_{\hat{b}_2}\xi$ for all $t \geq 0$, which implies that $\lim\limits_{t\to\infty}(\mathbf{n}(t) - \mathbf{n}^\star(t)) = \mathbf{0}$. ■

V. Control of $\mathbf{f}_{\mathbf{x}_1}(t,\mathbf{x}_1,\mathbf{u}_{\mathbf{x}_1})$ and of $\mathbf{f}_{\mathbf{x}_2}(t,\mathbf{x}_2,\mathbf{u}_{\mathbf{x}_2})$

In this Section, we provide control laws $\mathbf{u}_{\mathbf{x}_1}^{cl} \in \mathcal{C}(\mathbb{R}_{\geq 0} \times \Omega_{\mathbf{x}_1},\mathbb{R}^4)$ and $\mathbf{u}_{\mathbf{x}_2}^{cl} \in \mathcal{C}(\Omega_{\mathbf{x}_2},\mathbb{R}^3)$ that satisfy conditions of Assumption IV.1. However, we emphasize that Theorem IV.1 can be invoked for other functions than those suggested next.

A. Control of $\mathbf{f}_{\mathbf{x}_1}(t,\mathbf{x}_1,\mathbf{u}_{\mathbf{x}_1})$

The control law $\mathbf{u}_{\mathbf{x}_1}^{cl} \in \mathcal{C}(\mathbb{R}_{\geq 0} \times \Omega_{\mathbf{x}_1},\mathbb{R}^4)$ requires a controller $\mathbf{u}_{\bar{\boldsymbol{\xi}}}(\cdot)$ for a double integrator (where, along trajectories of $\ddot{\mathbf{p}}(t) = \mathbf{u}_{\bar{\boldsymbol{\xi}}}([\mathbf{p}^T(t)\,\dot{\mathbf{p}}^T(t)]^T)$, it is guaranteed that $\lim_{t\to\infty}\mathbf{p}(t) = \mathbf{0}$). The proposed control law $\mathbf{u}_{\bar{\boldsymbol{\xi}}}(\cdot)$ is that presented in [23] (Section V-A), which is inspired in [24]. This controller is bounded and it comes with a smooth Lyapunov function, two important facts that are exploited later.

Let us now present a possible control law $\mathbf{u}_{\mathbf{x}_1}^{cl} \in \mathcal{C}(\mathbb{R}_{\geq 0} \times \Omega_{\mathbf{x}_1},\mathbb{R}^4)$, which is based on the control strategy described in [25]. Consider the state $\mathbf{x}_1$ (see (9)), and denote $\bar{\boldsymbol{\xi}} = [\mathbf{e}^T\,\boldsymbol{\upsilon}^T]^T$. Consider then

$$\mathbf{T}^\star(t,\bar{\boldsymbol{\xi}}) := g\mathbf{e}_3 + \mathbf{p}_{cm}^\star(t) + \mathbf{u}_{\bar{\boldsymbol{\xi}}}(\bar{\boldsymbol{\xi}}), \mathbf{n}^\star(t,\bar{\boldsymbol{\xi}}) := \tfrac{\mathbf{T}^\star(t,\bar{\boldsymbol{\xi}})}{\|\mathbf{T}^\star(t,\bar{\boldsymbol{\xi}})\|},$$

$$\xi(t,\mathbf{x}_1) := 1 - \mathbf{n}^T\mathbf{n}^\star(t,\bar{\boldsymbol{\xi}})$$

$$\boldsymbol{\omega}^\star(t,\mathbf{x}_1) := \mathcal{S}\left(\mathbf{n}^\star(t,\bar{\boldsymbol{\xi}})\right)\tfrac{\frac{\partial \mathbf{T}^\star(t,\bar{\boldsymbol{\xi}})}{\partial t} + \frac{\partial \mathbf{T}^\star(t,\bar{\boldsymbol{\xi}})}{\partial \bar{\boldsymbol{\xi}}}^T(\mathbf{f}_{\bar{\boldsymbol{\xi}}}^{cl}(\bar{\boldsymbol{\xi}}) + \Pi(\mathbf{n})\mathbf{T}^\star(t,\bar{\boldsymbol{\xi}}))}{\|\mathbf{T}^\star(t,\bar{\boldsymbol{\xi}})\|}$$

where $\mathbf{u}_{\bar{\boldsymbol{\xi}}}(\cdot)$ and $V_{\bar{\boldsymbol{\xi}}}(\cdot)$ are found in [23]. From the above, we define the following control law

$$T^{cl}(t,\mathbf{x}_1) := \mathbf{n}^T\mathbf{T}^\star(t,\bar{\boldsymbol{\xi}}),$$

$$\boldsymbol{\omega}^{cl}(t,\mathbf{x}_1) := \boldsymbol{\omega}^\star(t,\mathbf{x}_1) - k_\theta\mathcal{S}\left(\mathbf{n}^\star(t,\bar{\boldsymbol{\xi}})\right)\mathbf{n} - \tfrac{\|\mathbf{T}^\star(t,\bar{\boldsymbol{\xi}})\|}{v_\theta}\mathcal{S}(\mathbf{n})\tfrac{\partial V_{\bar{\boldsymbol{\xi}}}(\bar{\boldsymbol{\xi}})}{\partial \boldsymbol{\upsilon}}.$$

$$\mathbf{u}_{\mathbf{x}_1}^{cl}(t,\mathbf{x}_1) := \begin{bmatrix} T^{cl}(t,\mathbf{x}_1) & \boldsymbol{\omega}^{cl,T}(t,\mathbf{x}) \end{bmatrix}^T. \quad (18)$$

For this control law $\mathbf{e}_1^T\mathbf{u}_{\mathbf{x}_1}^{cl}(\cdot,\cdot) = T^{cl}(\cdot,\cdot) \geq T_{\min}$, where $T_{\min} = g + \inf_{t\geq 0}\mathbf{e}_3^T\mathbf{p}_{cm}^\star(t) - \sup_{\bar{\boldsymbol{\xi}}\in\mathbb{R}^6}|\mathbf{e}_3^T\mathbf{u}_{\bar{\boldsymbol{\xi}}}(\bar{\boldsymbol{\xi}})| > 0$, and where the inequality is satisfied by properly tunning the controller $\mathbf{u}_{\bar{\boldsymbol{\xi}}}(\cdot)$ and by properly restricting $\mathbf{p}_{cm}^\star(\cdot)$.

Given $V_{\mathbf{x}_1} \in \mathcal{C}^2(\mathbb{R}_{\geq 0} \times \Omega_{\mathbf{x}_1},\mathbb{R}_{\geq 0})$ defined as $V_{\mathbf{x}_1}(t,\mathbf{x}_1) = V_{\bar{\boldsymbol{\xi}}}(\bar{\boldsymbol{\xi}}) + v_\theta\xi(t,\mathbf{x}_1)$, it follows that $W_{\mathbf{x}_1} \in \mathcal{C}^1(\mathbb{R}_{\geq 0} \times \Omega_{\mathbf{x}_1},\mathbb{R}_{\geq 0})$ is given by $W_{\mathbf{x}_1}(t,\mathbf{x}_1) = W_{\bar{\boldsymbol{\xi}}}(\bar{\boldsymbol{\xi}}) + v_\theta k_\theta\xi(t,\mathbf{x}_1)(2 - \xi(t,\mathbf{x}_1)) \geq 0$. Furthermore, notice that $\frac{\partial V_{\mathbf{x}_1}(t,\mathbf{x}_1)}{\partial \boldsymbol{\upsilon}} = \frac{\partial V_{\bar{\boldsymbol{\xi}}}(\bar{\boldsymbol{\xi}})}{\partial \boldsymbol{\upsilon}} + v_\theta\frac{\partial \xi(t,\mathbf{x}_1)}{\partial \boldsymbol{\upsilon}}$ which is used in (15).

B. Control of $\mathbf{f}_{\mathbf{x}_2}(\mathbf{x}_2,\mathbf{u}_{\mathbf{x}_2})$

Let us now focus on the control of the manipulator's orientation. Let us recall that the objective is that the manipulator tracks a desired orientation $\mathbf{n}^\star \in \mathcal{C}^2(\mathcal{S}^2)$. As such, it is necessary to construct a control law $\mathbf{u}_{\tilde{\mathbf{x}}}^{cl}(t,\mathbf{x}_2) = \boldsymbol{\alpha}^{cl}(t,\mathbf{x}_2)$ that guarantees that that objective is accomplished. For convenience, denote $\boldsymbol{\omega}^\star(t) = \mathcal{S}\left(\mathbf{n}^\star(t)\right)\dot{\mathbf{n}}^\star(t)$ and $\boldsymbol{\alpha}^\star(t) = \ddot{\mathbf{n}}^\star(t)$, and note that $\dot{\mathbf{n}}^\star(t) = \mathcal{S}\left(\boldsymbol{\omega}^\star(t)\right)\mathbf{n}^\star(t)$ and that $\dot{\boldsymbol{\omega}}^\star(t) = \mathcal{S}\left(\mathbf{n}^\star(t)\right)\boldsymbol{\alpha}^\star(t)$. Consider then $\mathbf{u}_{\mathbf{x}_2}^{cl} \in \mathcal{C}(\mathbb{R}_{\geq 0} \times \Omega_{\mathbf{x}_1},\mathbb{R}^3)$ defined as (denote $\Pi(\mathbf{x}) = \mathcal{S}(\mathbf{x})\,\mathcal{S}(\mathbf{x})^T$)

$$\begin{aligned}\mathbf{u}_{\mathbf{x}_2}^{cl}(t,\mathbf{x}_2) = \ & \mathcal{S}(\mathbf{n})\,\mathcal{S}\left(\mathbf{n}^\star(t)\right)^T\boldsymbol{\alpha}^\star(t) - k_\theta\tfrac{v_\theta}{v_\omega}\Pi(\mathbf{n})\,\mathbf{n}^\star(t) \\ & -\mathbf{n}^T\boldsymbol{\omega}^\star(t)\Pi(\mathbf{n})\left(\boldsymbol{\omega}^\star(t) - k_\theta\mathcal{S}\left(\mathbf{n}^\star\right)\mathbf{n}\right) \\ & -k_\omega\Pi(\mathbf{n})\left(\boldsymbol{\omega} - \boldsymbol{\omega}^\star(t) + k_\theta\mathcal{S}\left(\mathbf{n}^\star\right)\mathbf{n}\right) \\ & +\mathcal{S}(\mathbf{n})\left((\boldsymbol{\omega} - \boldsymbol{\omega}^\star(t))\mathbf{n}^T\mathbf{n}^\star(t) + \mathbf{n}^\star(t)\mathbf{n}^T\boldsymbol{\omega}^\star(t)\right),\end{aligned}$$

where k_θ, k_ω, v_θ and v_ω are positive constants. Consider also the Lyapunov function $V_{\mathbf{x}_2} \in \mathcal{C}^2(\mathbb{R}_{\geq 0} \times \Omega_{\mathbf{x}_1},\mathbb{R}_{\geq 0})$ defined as

$$\begin{aligned}V_{\mathbf{x}_2}(t,\mathbf{x}_2) = & v_\theta(1 - \mathbf{n}^T\mathbf{n}^\star(t)) + \\ & \tfrac{v_\omega}{2}\|\mathcal{S}(\mathbf{n})\left(\boldsymbol{\omega} - \boldsymbol{\omega}^\star(t) + k_\theta\mathcal{S}\left(\mathbf{n}^\star(t)\right)\mathbf{n}\right)\|^2.\end{aligned}$$

for which it follows that $W_{\mathbf{x}_2} \in \mathcal{C}^1(\mathbb{R}_{\geq 0} \times \Omega_{\mathbf{x}_1},\mathbb{R}_{\geq 0})$ is given by

$$\begin{aligned}W_{\mathbf{x}_2}(t,\mathbf{x}_2) = & v_\theta k_\theta(1 - \mathbf{n}^T\mathbf{n}^\star(t)) + \\ & v_\omega k_\omega\|\mathcal{S}(\mathbf{n})\left(\boldsymbol{\omega} - \boldsymbol{\omega}^\star(t) + k_\theta\mathcal{S}\left(\mathbf{n}^\star(t)\right)\mathbf{n}\right)\|^2.\end{aligned}$$

Furthermore, notice that $\frac{\partial V_{\mathbf{x}_2}(t,\mathbf{x}_2)}{\partial \boldsymbol{\omega}} = v_\omega\Pi(\mathbf{n})\left(\boldsymbol{\omega} - \boldsymbol{\omega}^\star(t) + k_\theta\mathcal{S}\left(\mathbf{n}^\star(t)\right)\mathbf{n}\right)$ which is used in (15).

VI. Simulations and Experiments

In this section, we present a simulation and two experiments that validate the proposed algorithms.

A. Simulation

Consider a quadrotor with mass $M = 1.442$ kg, a load with mass $m = 0.35$ kg, a manipulator with length $L = 0.35$ m, and a disturbance $b = 0.1$ N. Consider the control law $\mathbf{u}_{\bar{\boldsymbol{\xi}}}(\cdot)$ (in [23]) with $\sigma(s) = 0.25\frac{s}{\sqrt{1+s^2}}$, $\rho(s) = 0.70\frac{s}{\sqrt{1+s^2}}$, $k = 1$ and $\Omega(\cdot)$ as an odd function and as the solution to the differential equation $\Omega'''(s) = 1$ for $s > 1$ and $\Omega'''(s) = 0$ for $0 \leq s \leq 1$ and initial conditions $\Omega(0) = 0$, $\Omega'(0) = 1$ and $\Omega''(0) = 0$. Consider the control law $\mathbf{u}^{cl}_{\mathbf{x}_1}(\cdot,\cdot)$, in (18), with gains $v_\theta = 50$ and $k_\theta = 1$; the control law $\mathbf{u}^{cl}_{\mathbf{x}_2}(\cdot,\cdot)$, in (18), with gains $v_\theta = 20$, $k_\theta = 1$, $v_\omega = 20$ and $k_\omega = 1$. and, finally, the estimator vector field, in (15), with $k_{b_1} = 1$, $k_{b_2} = 0.05$, $b^{\max} = 0.3$ and $\epsilon = 0.1$. For these choices, we provide a simulation in Fig. 2, as a solution of (1) with $\mathbf{z}(0) = [-L\mathbf{e}_3^T\ \mathbf{0}^T\ \mathbf{0}^T\ \mathbf{0}^T\ \mathbf{e}_3^T]^T$. In Fig. 2(a), the desired trajectory is visualized in blue, specifically a quadrotor describing a circular motion of 1 m of radius and an angular velocity of 0.2 rev/sec, and with the manipulator describing a motion given by $\mathbf{n}^\star(t) = [0\ \sin(\gamma(t))\ \cos(\gamma(t))]$ with $\gamma(t) = \frac{\pi}{4}\cos(\frac{\pi}{5}t)$; while the actual trajectory of the quadrotor-manipulator system is visualized in black, where convergence to the desired trajectory is verified. In Fig. 2(b), the position tracking error of the quadrotor is presented, and it converges to $\mathbf{0}$; in Fig. 2(c), the thrust input, the quadrotor angular velocity and the disturbance estimate are presented; notice the disturbance estimate converges to the real unknown disturbance, namely 0.1N, thus canceling its effect. Finally, in Fig. 2(d), the orientation tracking error of the manipulator is presented, and it converges to 0; the torque input, as defined in (16), is also presented.

B. Experimental Set-up and Experiments

For the experiments, a commercial quadrotor was used, namely an IRIS+ from 3D Robotics, weighting 1.442 kg, with a maximum payload of 0.4kg. The commands for controlling the quadrotor are processed on a ground station, developed in a ROS environment, and sent to the on-board autopilot, which allows to remotely control the aerial vehicle through the total thrust and the angular velocity. A wireless radio communication between ground station and autopilot is established through a telemetry radio, using a MAVLink protocol that directly overrides the signals sent from the radio transmitter. The quadrotor's pose is estimated by 12 cameras from a Qualisys motion capture system.

Three experiments were conducted, with a manipulator rigidly attached to the quadrotor. The manipulator consists of a rigid bar, of 0.35m of length and with a load at the extremity of 0.355kg – for this manipulator, the center of mass of the quadrotor-manipulator system shifts by approximately 7 cm away from the quadrotor center of mass. For the three experiments, the controller has the same structure, specifically that in (18) and the desired trajectory is the same. In the first experiment, trajectory tracking of the center of mass of the quadrotor-manipulator system is performed – Fig. 3(a); in the second, trajectory tracking of the center of mass of the quadrotor without manipulator is performed – Fig. 3(b); and, in the third, trajectory tracking of the center of mass of the quadrotor, but where the manipulator is attached and where the controller is oblivious to its presence, is performed – Fig. 3(c). For the first two experiments, the tracking performance and behavior is good as expected. However, for the third experiment, the tracking performance is slightly worse, with slower convergence to the steady state and some extra oscillations around the steady state, when compared to the previous two experiments; in this case, the manipulator is present but it is seen as a disturbance on the system, which explains the decrease in performance. This indicates that considering the manipulator presence, as done in the first experiment, can benefit the tracking performance.

A pick-and-place task experiment was also performed – Fig. 4. First, the quadrotor moves over the target point – target 1, it descends and it grasps the object at the picking position; once the object is grasped, the quadrotor goes back to the initial altitude and it moves to the target point – target 2; at the target point, the quadrotor descends and drops the object. When the load is grasped or released, the controller is updated, and the center of mass is recomputed before a new desired trajectory is set. Figure 4(a) shows that the task is successfully accomplished. During the descent phase the robot's actual trajectory leaves the tolerance region in two occasions. In particular, when the vehicle is close to the picking or dropping place, the propellers airflow causes turbulence which disturbs the dynamics of the system. However, as seen in Figure 4(a) and Figure 4(b), the algorithm pauses the descent phase until the position error returns within the tolerance region. A companion video with experiments – different runs but same conditions as the experiments described before – is found that illustrates both this and the previous experiment.

References

[1] AEROWORKS aim. http://www.aeroworks2020.eu/.

[2] M. Hua, T. Hamel, P. Morin, and C. Samson. Introduction to feedback control of underactuated VTOL vehicles: A review of basic control design ideas and principles. *Control Systems*, 33(1):61–75, 2013.

[3] P. Cruz and R. Fierro. Autonomous lift of a cable-suspended load by an unmanned aerial robot. In *Conference on Control Applications*, pages 802–807. IEEE, 2014.

[4] I. Palunko, R. Fierro, and P. Cruz. Trajectory generation for swing-free maneuvers of a quadrotor with suspended payload: A dynamic programming approach. In *International Conference on Robotics and Automation*, pages 2691–2697. IEEE, 2012.

[5] M. Bisgaard, A. la Cour-Harbo, and J. D. Bendtsen. Adaptive control system for autonomous helicopter slung load operations. *Control Engineering Practice*, 18(7):800–811, 2010.

[6] N. Michael, J. Fink, and V. Kumar. Cooperative manipulation and transportation with aerial robots. *Autonomous Robots*, 30(1):73–86, 2011.

[7] D. Mellinger, Q. Lindsey, M. Shomin, and V. Kumar. Design, modeling, estimation and control for aerial grasping and manipulation. In *IEEE/RSJ IROS*, pages 2668–2673. IEEE, 2011.

[8] P. Pounds, D. Bersak, and A. Dollar. Grasping from the air: Hovering capture and load stability. In *International Conference on Robotics and Automation*, pages 2491–2498. IEEE, 2011.

[9] J. Thomas, J. Polin, K. Sreenath, and V. Kumar. Avian-inspired grasping for quadrotor micro UAV's. In *ASME 2013 International Design Engineering Technical Conferences and Computers and Information in Engineering Conference*, 2013.

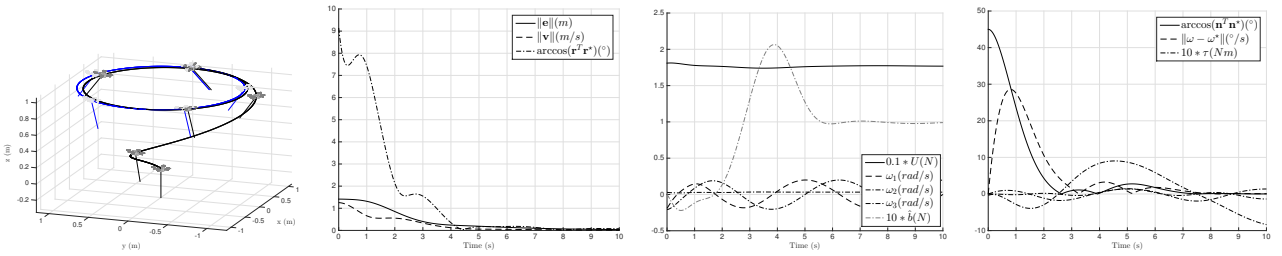

(a) Trajectories

(b) Position tracking error and attitude error of quadrotor

(c) Thrust input, angular velocity and disturbance estimate

(d) Manipulator errors and torque inputs

Fig. 2: Simulation for $\mathbf{z}(0) = [-L\mathbf{e}_3^T \ \mathbf{0}^T \ \mathbf{0}^T \ \mathbf{0}^T \ \mathbf{e}_3^T]^T$.

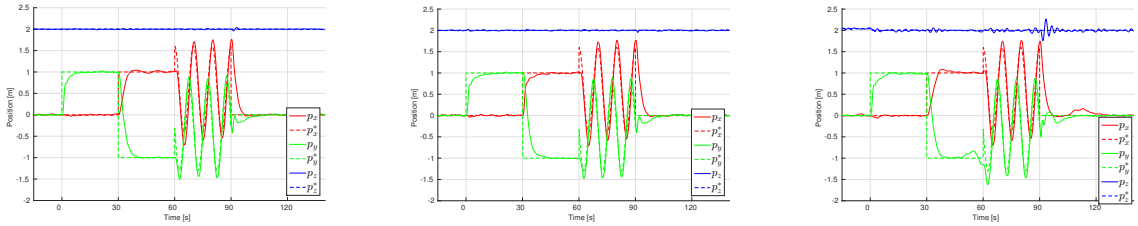

(a) Tracking of center of mass of quadrotor-manipulator system.

(b) Tracking of center of mass of quadrotor system, without manipulator.

(c) Tracking of center of mass of quadrotor system, with manipulator attached (control oblivious to manipulator presence).

Fig. 3: Position trajectory tracking for different configurations, with controller defined in 18

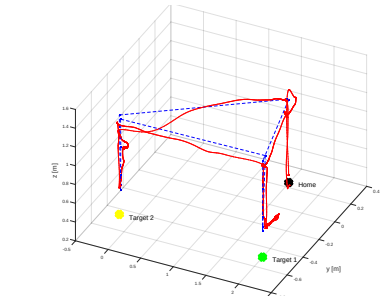

(a) Blue: desired trajectory. Red: real trajectory. Target 1 is the picking point, and Target 2 is the dropping point.

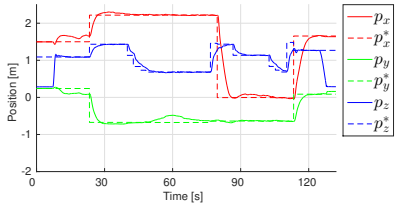

(b) Tracking error during flight.

Fig. 4: Pick and place experiment

[10] D. Mellinger, M. Shomin, N. Michael, and V. Kumar. Cooperative grasping and transport using multiple quadrotors. In *Distributed autonomous robotic systems*, pages 545–558. Springer, 2013.

[11] F. et al Huber. First analysis and experiments in aerial manipulation using fully actuated redundant robot arm. In *International Conference on Intelligent Robots and Systems*, pages 3452–3457. IEEE, 2013.

[12] A. Jimenez-Cano, J. Martin, G. Heredia, A. Ollero, and R. Cano. Control of an aerial robot with multi-link arm for assembly tasks. In *International Conference on Robotics and Automation*, pages 4916–4921. IEEE, 2013.

[13] C. Korpela, M. Orsag, M. Pekala, and P. Oh. Dynamic stability of a mobile manipulating unmanned aerial vehicle. In *International Conference on Robotics and Automation*, pages 4922–4927, 2013.

[14] J. Escareno, G. Flores, M. Rakotondrabe, H. Romero, R. Lozano, and E. Rubio. Task-based control of a multirotor miniature aerial vehicle having an onboard manipulator. In *International Conference on Unmanned Aircraft Systems*, pages 857–863. IEEE, 2014.

[15] F. Ruggiero et al. A multilayer control for multirotor UAVs equipped with a servo robot arm. In *International Conference on Robotics and Automation*, pages 4014–4020. IEEE, 2015.

[16] S. Kannan, M. Alma, M. Olivares-Mendez, and H. Voos. Adaptive control of aerial manipulation vehicle. In *International Conference on Control System, Computing and Engineering*, pages 273–278. IEEE, 2014.

[17] G. Antonelli and E. Cataldi. Adaptive control of arm-equipped quadrotors. theory and simulations. In *Mediterranean Conference of Control and Automation*, pages 1446–1451. IEEE, 2014.

[18] V. Lippiello and F. Ruggiero. Exploiting redundancy in cartesian impedance control of uavs equipped with a robotic arm. In *IEEE/RSJ IROS*, pages 3768–3773. IEEE, 2012.

[19] J. Acosta, M.I. Sanchez, and Aníbal Ollero. Robust control of underactuated aerial manipulators via IDA-PBC. In *Conference on Decision and Control*, pages 673–678. IEEE, 2014.

[20] J. Escareno, M. Rakotondrabe, G. Flores, and R. Lozano. Rotorcraft MAV having an onboard manipulator: Longitudinal modeling and robust control. In *ECC*, pages 3258–3263, 2013.

[21] S. Kim, S. Choi, and H. Kim. Aerial manipulation using a quadrotor with a two dof robotic arm. In *International Conference on Intelligent Robots and Systems*, pages 4990–4995. IEEE, 2013.

[22] Z. Cai, M.S. de Queiroz, and D.M. Dawson. A sufficiently smooth projection operator. *Transactions on Automatic Control*, 51(1):135–139, Jan 2006.

[23] P. Pereira, M. Herzog, and D. V. Dimarogonas. Slung load transportation with single aerial vehicle and disturbance removal. In *24th Mediterranean Conference on Control and Automation*, pages 671–676, 2016.

[24] Frédéric Mazenc and Abderrhaman Iggidr. Backstepping with bounded feedbacks. *Systems & control letters*, 51(3):235–245, 2004.

[25] P.O. Pereira and D.V. Dimarogonas. Lyapunov-based generic controller design for thrust-propelled underactuated systems. In *European Control Conference*, pages 594–599, 2016.